Applied Probability Trust (23 March 2010)

PROBABILISTIC RESULTS FOR A MOBILE SERVICE SCENARIO

JESPER MØLLER,[*] *Aalborg University*

MAN LUNG YIU,[**] *Hong Kong Polytechnic University*

Abstract

We consider the following stochastic model for a mobile service scenario. Consider a stationary Poisson process in $\mathbb{R}^d$, with its points radially ordered with respect to the origin (the anchor); if $d = 2$, the points may correspond to locations of e.g. restaurants. A user, with a location different from the origin, asks for the location of the first Poisson point and keeps asking for the location of the next Poisson point until the first time that he can be completely certain that he knows which Poisson point is his nearest neighbour. This waiting time is the communication cost, while the inferred privacy region is a random set obtained by an adversary who only knows the anchor and the points received from the server, where the adversary 'does the best' to infer the possible locations of the user. Probabilistic results related to the communication cost and the inferred privacy region are established for any dimension $d \geq 1$. Furthermore, special results when $d = 1$ and particularly when $d = 2$ are derived.

Keywords: communication cost; nearest-neighbour search; Poisson process; privacy region; radial simulation algorithm; Voronoi tessellation

AMS 2000 Subject Classification: Primary 60D05;60G55;62M30
Secondary 68U20

[*] Postal address: Department of Mathematical Sciences, Aalborg University Fredrik Bajers Vej 7G, DK-9220 Aalborg, Denmark. Email address: jm@math.auc.dk

[**] Postal address: Department of Computing Hong Kong Polytechnic University Hung Hom, Kowloon Hong Kong. Email address: csmlyiu@comp.polyu.edu.hk

1. Introduction

The mobile Internet offers services that e.g. receive the location of the nearest point of interest such as a store, restaurant, or tourist attraction, see [9, 10] and the references therein. This paper demonstrates that tools from applied probability and in particular stochastic geometry can be useful when analysing the performance of such services.

The paper considers a setting for a mobile service protocol proposed by [9, 10], where a user is located at a point $q \in \mathbb{R}^d$ and a stationary Poisson point process $\Phi = \{X_1, X_2, \ldots\} \subset \mathbb{R}^d$ is given; for the problem setting in [9, 10], $d = 2$ and the points in Φ may e.g. correspond to the locations of stores. In order to preserve some privacy, the user queries a server for nearby points in Φ but he reports not his correct location q but another location $q' \in \mathbb{R}^d$ referred to as the anchor. An incremental query processing on the server is used so that the points $X_1, X_2, \ldots$ are ordered in increasing distance to the anchor. The user then stops to query the server as soon as possible, i.e., when the nearest point in Φ with respect to q can be determined. The waiting time for this to happen is called the communication cost and is denoted M. Another object of interest is the inferred privacy region, which is a random set $\mathcal{R} \subset \mathbb{R}^d$ obtained by an adversary who only knows the location of the anchor and the points received from the server, where the adversary 'does the best' to infer the possible locations of the user. The precise definitions of M and $\mathcal{R}$ are given in Sections 2 and 3, respectively.

The assumption that Φ is a stationary Poisson process is motivated by that this is the most fundamental spatial point process model in stochastic geometry, and it often serves as a natural starting point for statistical analysis, see, e.g., [1, 4, 8]. Our objective is to analyse the distribution of M and various properties of $\mathcal{R}$, where we exploit the independence properties of the Poisson process to derive analytical results; for other point process models Monte Carlo simulations will probably be needed. In Section 2, the distribution and moments for M are derived in detail. Section 3 describes first the geometric properties of $\mathcal{R}$, and second establishes results related to the probability that $\mathcal{R}$ contains a given point in $\mathbb{R}^d$ and the expected value of V, where $V = |\mathcal{R}|$ is the d-dimensional volume of the inferred privacy region.

2. The communication cost

2.1. Preliminaries

2.1.1. *Assumptions:* Denote $l = \|q - q'\|$ the distance between the anchor and the user location, and $R_i = \|X_i - q'\|$ the distance of X_i to q'. The case where $l = 0$ turns out to be trivial since Φ is a stationary Poisson process, so we assume that $l > 0$. Any point X_i in Φ is a random variable, and we order the points in Φ such that $R_0 := 0 \leq R_1 \leq R_2 \leq \ldots$. Note that these inequalities are strict almost surely, and we let $U_i = (X_i - q')/R_i$ be the unit vector specifying the direction from q' to X_i (provided $R_i > 0$). Denote Z the nearest neighbour to q among $X_1, X_2, \ldots$. For $i = 1, 2, \ldots$, let Q_i be the nearest neighbour to q among the i first points $X_1, \ldots, X_i$, and set $D_i = \|q - Q_i\|$ (so Z and Q_i are almost surely uniquely defined). Denote $B(x, r) = \{y \in \mathbb{R}^d : \|y - x\| \leq r\}$ the closed ball in $\mathbb{R}^d$ with centre $x \in \mathbb{R}^d$ and radius $r \geq 0$. Let $|\cdot|$ denote volume (Lebesgue measure) in $\mathbb{R}^d$, and

$$\omega_d = |B(0,1)| = \pi^{d/2}/\Gamma(1 + d/2)$$

the volume of the d-dimensional unit ball. Finally, denote $\rho > 0$ the intensity of Φ and define

$$\alpha = (\rho |B(0,l)|)^{1/d} = (\omega_d \rho)^{1/d}\, l.$$

2.1.2. *Radial simulation algorithm:* We can easily generate any number of points from Φ using a radial simulation algorithm due to Quine and Watson [6] and based on the following properties.

(I) $R_1^d, R_2^d, \ldots$ form a homogeneous Poisson process on the positive halfline with intensity $\omega_d \rho$, i.e., $R_1^d - R_0^d, R_2^d - R_1^d, \ldots$ are independent and exponentially distributed with mean $1/(\omega_d \rho)$;

(II) the sequence $R_1^d, R_2^d, \ldots$ is independent of the sequence $U_1, U_2, \ldots$;

(III) the U_i are independent and uniformly distributed on the unit sphere in $\mathbb{R}^d$.

2.1.3. *Definition of the communication cost:* Denote $\mathbb{N} = \{1, 2, \ldots\}$ the set of positive integers. For $i \in \mathbb{N}$, define the *demand space* by $\mathcal{D}_i = B(q, D_i)$ and the *supply space* by $\mathcal{S}_i = B(q', R_i)$. Then $(\mathcal{D}_i)_{i \in \mathbb{N}}$ is decreasing, $(\mathcal{S}_i)_{i \in \mathbb{N}}$ is increasing, and we define the *communication cost* as the discrete random variable M given by the first time the demand space is included in the supply space, that is,

$$M = \inf\{i \in \mathbb{N} : \mathcal{D}_i \subseteq \mathcal{S}_i\} \tag{1}$$

(setting $\inf \emptyset = \infty$). See Figure 1. In other words, for any $m \in \mathbb{N}$, $M = m$ if m is the first time the user can be completely ensured that $Z = Q_m$ when he has only received $X_1, \ldots, X_m$ from the server, i.e., no matter where the points $X_{m+1}, X_{m+2}, \ldots$ potentially could be located in $\mathbb{R}^d \setminus B(q', R_m)$. Note that M is almost surely finite (this is verified in Lemma 1 below), in which case

$$Z = Q_M \tag{2}$$

is returned as the nearest neighbour to q.

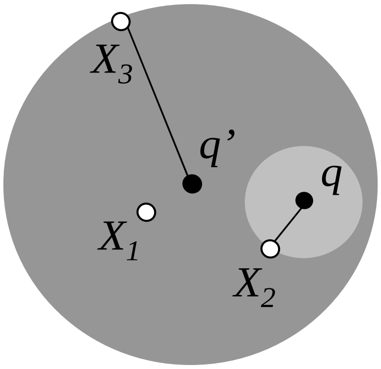

FIGURE 1: An planar example ($d = 2$) with $M = 3$ and showing the corresponding demand space $\mathcal{D}_3$ and supply space $\mathcal{S}_3$. Note that $\mathcal{D}_2 = \mathcal{D}_3$ and $Z = Q_2 = Q_3$.

2.2. Results

For $d \geq 2$, we can exclude certain events of zero probability and thereby simplify the meaning of M and Z as stated in the following lemma, where it should be noticed that we have strict inclusion in (3); compare (3) with (1) and Figure 1.

Lemma 1. *For $d \geq 2$, with probability one,*

$$M = \inf\{m \in \{2, 3, \ldots\} : \mathcal{D}_{m-1} \subset \mathcal{S}_m\} < \infty \tag{3}$$

and

$$Z = Q_M = Q_{M-1}, \quad D_M = D_{M-1}, \quad R_M \geq l. \tag{4}$$

Proof. Clearly, by (1), $R_M \geq l$. Since $M = 1$ implies that X_1 lies on the halfline H with endpoint q and direction $q - q'$, and this happens with probability zero, we have almost surely that $M \geq 2$. Further, with probability one, for $m \in \{2, 3, \ldots\}$, $M = m$ implies that $Q_m \neq X_m$ because $Q_m = X_m$ would imply that $X_m \in H$ which happens with probability zero. Moreover, with probability one, the sequence $R_1, R_2, \ldots$ is strictly increasing to infinity, and so the sequence of supply spaces $\mathcal{S}_1 \subset \mathcal{S}_2 \subset \ldots$ tends to $\mathbb{R}^d$. On the other hand, the sequence of demand spaces decreases. Combining these facts with (1) and (2), we obtain that (3) and (4) hold almost surely.

Let $T = \|Z - q\|$ be the distance from the user to its nearest point in Φ, and let $\Psi = \Phi \cap [B(q', T+l) \setminus B(q, T)]$ be the restriction of Φ to the random set $B(q', T+l) \setminus B(q, T)$. Let N denote the number of points in Ψ, and set $S = \omega_d \rho T^d$ and

$$\Lambda = \rho |B(q', l + T) \setminus B(q', T)| = \left(\alpha + S^{1/d}\right)^d - S = \sum_{i=0}^{d-1} \binom{d}{i} \alpha^{d-i} S^{i/d}. \tag{5}$$

Since Φ is a Poisson process, we obtain that

(i) S is exponentially distributed with parameter one;

(ii) conditional on Z, $\Phi \setminus B(q, T)$ is a homogeneous Poisson process on $\mathbb{R}^d \setminus B(q, T)$ with intensity ρ, and Ψ is a homogeneous Poisson process on $B(q', T+l) \setminus B(q, T)$ with its mean number of points equal to Λ;

(iii) in the special case $d = 1$, the event $Z = X_M$ is equivalent to that $Z - q$ has the same sign as $q - q'$, so $\mathrm{P}(Z = X_M) = 1/2$, and if $Z = X_M$ then $N = M - 1$ and $\Psi = \{X_1, \ldots, X_{M-1}\}$, while if $Z \neq X_M$ then $N = M - 2$ and $\Psi = \{X_1, \ldots, X_{M-1}\} \setminus \{Z\}$;

(iv) for $d \geq 2$, with probability one, $N = M - 2$ and $\Psi = \{X_1, \ldots, X_{M-1}\} \setminus \{Z\}$, cf. Lemma 1.

These results are now used to obtain the distribution of N (or equivalently M), where $\mathrm{po}(\alpha)$ denotes the Poisson distribution with parameter α.

Theorem 1. *(a) For $d = 1$, N is independent of Z and follows* $\mathrm{po}(\alpha)$*,*

$$\mathrm{P}(M=1) = \frac{\mathrm{e}^{-\alpha}}{2}, \quad \mathrm{P}(M=m) = \left(\frac{\alpha^{m-1}}{(m-1)!} + \frac{\alpha^{m-2}}{(m-2)!}\right)\frac{\mathrm{e}^{-\alpha}}{2}, \quad m = 2,3,\ldots, \tag{6}$$

and M has mean and variance

$$\mathrm{E}(M) = \alpha + 3/2, \quad \mathrm{V}(M) = \alpha + 1/4, \tag{7}$$

with $\alpha = 2\rho l$.

(b) For $d = 2$,

$$\mathrm{P}(M=m) = \int_0^\infty \frac{\left(\alpha^2 + 2\alpha\sqrt{s}\right)^{m-2}}{(m-2)!}\mathrm{e}^{-\left(\alpha^2+2\alpha\sqrt{s}+s\right)}\,\mathrm{d}s, \quad m = 2,3,\ldots, \tag{8}$$

and

$$\mathrm{E}(M) = \alpha^2 + \sqrt{\pi}\alpha + 2, \quad \mathrm{V}(M) = (5-\pi)\alpha^2 + \sqrt{\pi}\alpha, \tag{9}$$

with $\alpha = \sqrt{\pi\rho}\, l$.

(c) For $d \geq 2$, $M - 2$ conditional on Z follows $\mathrm{po}(\Lambda)$*, and*

$$\mathrm{E}(M) = 2 + \sum_{i=0}^{d-1}\binom{d}{i}\alpha^{d-i}\Gamma\left(1+\frac{i}{d}\right), \tag{10}$$

$$\begin{aligned}\mathrm{V}(M) = {} & \sum_{i=0}^{d-1}\binom{d}{i}\alpha^{d-i}\Gamma\left(1+\frac{i}{d}\right) \\ & + \sum_{i=1}^{d-1}\sum_{j=1}^{d-1}\binom{d}{i}\binom{d}{j}\alpha^{2d-i-j}\left[\Gamma\left(1+\frac{i+j}{d}\right) - \Gamma\left(1+\frac{i}{d}\right)\Gamma\left(1+\frac{j}{d}\right)\right]. \end{aligned}\tag{11}$$

(d) For $d \geq 1$ and any number β, $\mathrm{E}(M^\beta) < \infty$.

Proof. If $d = 1$, since $\Lambda = \alpha$ is then deterministic, (ii) implies that N is independent of Z and follows $\mathrm{po}(\alpha)$. Hence (iii) easily implies (6) and (7), and so (a) follows.

If $d \geq 2$, then by (ii), N conditional on Z follows $\mathrm{po}(\Lambda)$, and by (iv), $M = N + 2$, so $\mathrm{E}(M) = 2 + \mathrm{E}(\Lambda)$ and

$$\mathrm{V}(M) = \mathrm{V}(N) = \mathrm{E}(\mathrm{V}(N|\Lambda)) + \mathrm{V}(\mathrm{E}(N|\Lambda)) = \mathrm{E}(\Lambda) + \mathrm{V}(\Lambda).$$

Combining this with (5) and that by (i), $\mathrm{E}(S^\beta) = \Gamma(\beta+1)$ for $\beta > -1$, we obtain after a straightforward calculation that (10) and (11) hold for $d \geq 2$, where (9) is the case with $d = 2$. Then (8) immediately follows by combining (5), (i), and the fact that N conditional on S follows $\mathrm{po}(\Lambda)$. Thereby (b)-(c) are verified.

For $\beta \leq 0$, $M^\beta \leq 1$, and so (d) clearly holds. For $\beta > 0$, (d) follows immediately from (a) if $d = 1$, and from (c) and (5) if $d \geq 2$, using again that $\mathrm{E}(S^\beta) = \Gamma(\beta + 1)$. Hence (d) is verified.

Suppose $d = 2$ and let $\mathrm{erf}(\alpha) = (2/\sqrt{\pi}) \int_0^\alpha \exp(-t^2)\, \mathrm{d}t$ be the 'error function'. Then (8) gives

$$\mathrm{P}(M = 2) = \exp(-\alpha^2) + \alpha\sqrt{\pi}(\mathrm{erf}(\alpha) - 1),$$

which strictly decreases from one to zero as α decreases from zero to infinity. We have also evaluated the integral in (8) for $m = 3, 4, \ldots$ using the computational software program Maple, but since the number of terms increases fast as m increases we omit the results here. By (5) and (c), $M - 2$ conditional on S follows $\mathrm{po}(\alpha^2 + 2\alpha\sqrt{S})$. Hence, as $\alpha \to \infty$, $(M/\alpha) - \alpha$ converges in distribution to a mixture of normal distributions with mean $2\sqrt{S}$ and unit variance.

3. The inferred privacy region

3.1. Preliminaries

3.1.1. *Definition of the inferred privacy region* Suppose that an adversary knows the location q' of the anchor, the termination conditions (1)-(2), the termination time M, and the points $X_1, \ldots, X_M$ received from the server, while the location q of the user is unknown to him. If the adversary then wants to infer the possible locations of q, the best the adversary can do is to estimate q to be contained in the inferred privacy region which is a random set $\mathcal{R}$ specified below.

Consider the Voronoi tessellation of $\mathbb{R}^d$ generated by $\{X_1, \ldots, X_M\}$, with cells

$$C_i = \{x \in \mathbb{R}^d : \|x - X_i\| \leq \|x - X_j\|, j = 1, \ldots, M\}, \quad i = 1, \ldots, M.$$

The Voronoi cells have disjoint interiors with boundaries of zero volume (with respect to Lebesgue measure in $\mathbb{R}^d$), and with probability one they are d-dimensional sets [3, 5]. Note that $B(x, \|x - X_i\|) \subseteq B(q', r)$ if and only if $\|x - q'\| + \|x - X_i\| \leq r$. Consequently, if $M \geq 2$ and $i \in \{1, \ldots, M - 1\}$, the set

$$E_i = \{x \in C_i : R_{M-1} < \|x - q'\| + \|x - X_i\| \leq R_M\} \tag{12}$$

consists 'essentially' of all possible locations x of the user such that X_i is returned under the termination conditions as the nearest neighbour to x. By 'essentially' we mean that if x is on the boundary of C_i so that $x \in C_j$ for some $j < i$, then X_i would not had been returned, but the set of such points x has zero volume and as argued in comment (E) below, it plays no important rule but is just convenient that we have included such points in E_i. Moreover, the set of all possible locations $x \in C_M \setminus \cup_{i=1}^{M-1} C_i$ of the user is given by

$$E_M = [q', X_M] \setminus \bigcup_{i=1}^{M-1} C_i, \tag{13}$$

where $[q', X_M]$ is the closed line segment with end points q' and X_M, and we set $\cup_{i=1}^{M-1} C_i = \emptyset$ if $M = 1$. The *inferred privacy region* is therefore given by

$$\mathcal{R} = \bigcup_{i=1}^{M} E_i. \tag{14}$$

Figure 2 shows an example of $\mathcal{R}$ when $d = 2$ and the points are generated by the radial simulation algorithm in Section 2.1.2.

3.1.2. *Comments:* Some remarks are in order.

(A) If $M = 1$ then simply $\mathcal{R} = E_M = [q', X_M]$.

(B) If $1 \le i \le M - 1$ then by (12), $E_i = C_i \cap (F_i \setminus G_i)$, where F_i and G_i are the ellipsoidal regions with foci q' and X_i, such that any point on the boundary has its sum of distances to the foci equal to R_M and R_{M-1}, respectively (see cells $1, \dots, 15$ in Figure 2). As illustrated in Figure 2, E_i can be a connected set (see e.g. cell 1) or a disconnected set (see cell 9) or the empty set (see e.g. cell 3), $G_{M-1} = [q', X_{M-1}]$ is a closed line segment (see cell 15), while for $1 \le i \le M-2$, F_i and G_i are almost surely of dimension d.

(C) If $M \ge 2$ then E_M is the line segment given by the intersection of $[q', X_M]$ and the interior of C_M, cf. (13) (see cell 16 in Figure 2).

(D) If $d \ge 2$, E_M has zero d-dimensional volume, and the adversary could exclude both the possibility that $M = 1$ and the possibility that X_M is the nearest point in Φ to the user, since the event that $M = 1$ or $x \in [q, X_M]$ has probability zero.

(E) Recalling the considerations in connection to (12) concerning the boundary points of the Voronoi cells, note that $\mathcal{R} = \cup_{i=1}^{M} E_i'$, where $E_i' = E_i \setminus \cup_{j=1}^{i-1} C_j$ is exactly

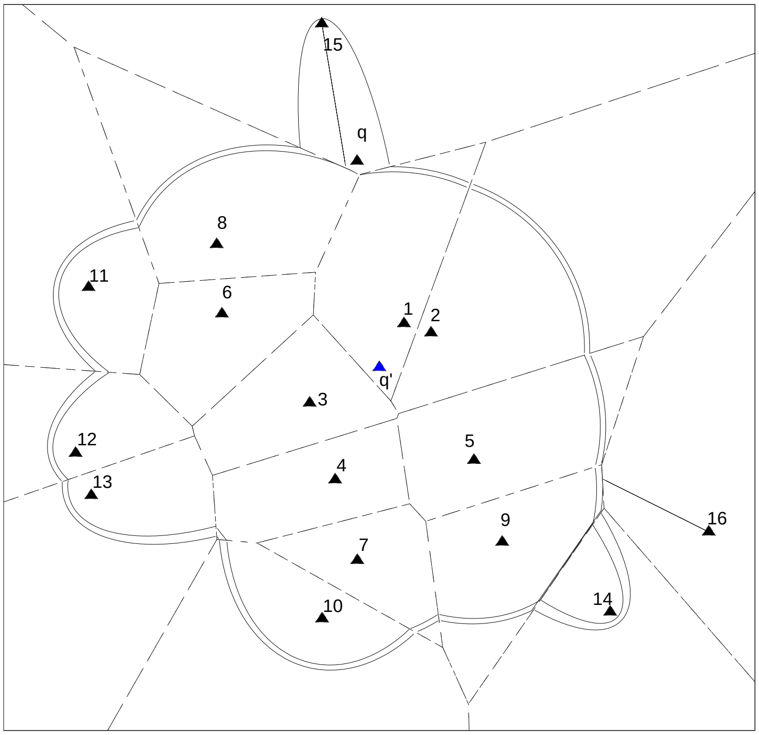

Figure 2: A planar inferred privacy region $\mathcal{R}$ (the solid lines except those on the boundary of the square) defined by $M = 16$ points (the triangles marked $1, \dots, 16$) and the anchor q'. The Voronoi tessellation with nuclei $X_1, \dots, X_M$ is shown as dotted lines. Also the user location q is shown, but the inferred privacy region is unchanged if any other point in $\mathcal{R}$ had been the location of the user.

the set of all possible locations x of the user such that X_i is returned under the termination conditions as the nearest neighbour to x (setting $\cup_{j=1}^{i-1} C_j = \emptyset$ if $i = 1$). Clearly, $E_i \setminus E_i'$ has zero volume.

3.2. Results

The volume of the inferred privacy region, $V = |\mathcal{R}|$, is a 'measure of privacy' with mean value

$$\mathrm{E}(V) = \int p(x)\,\mathrm{d}x, \tag{15}$$

where for any location $x \in \mathbb{R}^d$,

$$p(x) = \mathrm{P}(x \in \mathcal{R})$$

is the probability that x is in the inferred privacy region. Writing $Z = q + TU$, then U is a uniformly distributed unit vector in $\mathbb{R}^d$, T and U are independent, and T^d is exponentially distributed with rate $\rho\omega_d$, so Z has density function

$$f(z) = \rho \exp\left(-\rho\omega_d \|z - q\|^d\right). \tag{16}$$

Our strategy is first to determine the conditional probability

$$p(x|z) = \mathrm{P}(x \in \mathcal{R}|Z = z),$$

second to calculate

$$p(x) = \int p(x|z) f(z)\,\mathrm{d}z, \tag{17}$$

and finally to obtain $\mathrm{E}(V)$ from (15).

For any number s and set $A \subseteq \mathbb{R}^d$, define $sA = \{sa : a \in A\}$ and $q' + A = \{q' + a : a \in A\}$. To stress that the distribution of $\mathcal{R}$ and V depend only on (q', ρ, l) and (ρ, l), respectively, write $\mathcal{R}_{(q',\rho,l)}$ for $\mathcal{R}$, and $V_{(\rho,l)}$ for V. Let $\mathcal{R}_{(\rho,l)} = \mathcal{R}_{(o,\rho,l)}$ be the case with $q' = o$, the origin in $\mathbb{R}^d$, and note that $\mathcal{R}_{(q',\rho,l)} \sim q' + \mathcal{R}_{(\rho,l)}$, where $\sim$ means 'is distributed as'. Since $(1/l)\Phi$ is a Poisson process with intensity ρl^d, we obtain the following scaling properties,

$$\mathcal{R}_{(\rho,l)} \sim l\mathcal{R}_{(\rho l^d,1)}, \quad V_{(\rho,l)} \sim l^d V_{(\rho l^d,1)}. \tag{18}$$

Consequently, for distributional properties of the inferred privacy region and in particular for calculating $\mathrm{E}V$, it suffices to consider the case with $l = 1$ and $q' = o$.

In the remainder of this paper, we restrict attention to finding $p(x)$ and $\mathrm{E}V$ when $d \geq 2$. Theorem 2 below establishes an expression of $p(x|z)$; similar techniques apply in the special case $d = 1$, but the details are then somewhat more complicated since we have to account for each of the cases where $Z = X_M$ and $Z \neq X_M$, cf. (iii) (above Theorem 1).

Let $\mathbf{1}[\cdot]$ denote the indicator function. For $x, y \in \mathbb{R}^d$ and $r, s, t \geq 0$, define

$$c(r, s, t) = |B(x, s) \cap B(y, t)| \quad \text{if } r = \|x - y\|$$

and

$$\begin{aligned}
p(x,y,t) = {}& \mathbf{1}[\|x-q'\| + \|y-x\| \geq t+l] \exp\bigg(- \rho\{\omega_d[(\|x-q'\| + \|y-x\|)^d - (t+l)^d] \\
& - c(\|x-q'\|, t+l, \|y-x\|) + c(\|x-q\|, t, \|y-x\|)\}\bigg) \\
& + \mathbf{1}[\|x-q'\| + \|y-x\| < t+l] \exp\bigg(- \rho\big\{\omega_d\big[(t+l)^d - t^d - (\|x-q'\| + \|y-x\|)^d \\
& + \|y-x\|^d\big] + c(l, t, \|x-q'\| + \|y-x\|) - c(\|x-q\|, t, \|y-x\|)\big\}\bigg). \qquad (19)
\end{aligned}$$

Note that $c(r,s,t) = 0$ if $r \geq s+t$ or $s=0$ or $t=0$, and $c(r,s,t) = \omega_d \min\{s^d, t^d\}$ if $r=0$. If $d=2$, $r < s+t$, and $r,s,t > 0$, then

$$\begin{aligned}
c(r,s,t) = {}& s^2 \arccos\left(\frac{r^2+s^2-t^2}{2rs}\right) - \frac{r^2+s^2-t^2}{4r^2}\left[4r^2s^2 - \left(r^2+s^2-t^2\right)^2\right]^{1/2} \\
& + t^2 \arccos\left(\frac{r^2+t^2-s^2}{2rt}\right) - \frac{r^2+t^2-s^2}{4r^2}\left[4r^2t^2 - \left(r^2+t^2-s^2\right)^2\right]^{1/2}.
\end{aligned}$$

Theorem 2. *For $d \geq 2$ and $x, z \in \mathbb{R}^d$, letting $t = \|z-q\|$, then*

$$\begin{aligned}
& p(x|z) = p(x,z,t) + \\
& \rho \int \mathbf{1}\left[y \in B(q', t+l) \setminus B(q,t),\, z \in B(q', \|x-q'\| + \|y-x\|) \setminus B(x, \|y-x\|)\right] \\
& p(x,y,t)\,\mathrm{d}y. \qquad (20)
\end{aligned}$$

Proof. We start by verifying that

$$p(x,y,t) = p_1(x,y,t)p_2(x,y,t), \qquad (21)$$

where

$$p_1(x,y,t) = \exp\left(-\rho\omega_d \max\{0, (\|x-q'\| + \|y-x\|)^d - (t+l)^d\}\right)$$

and

$$\begin{aligned}
& p_2(x,y,t) = \\
& \quad \exp\bigg(- \rho|\{B(q', t+l) \setminus B(q,t)\} \setminus \{B(q', \|x-q'\| + \|y-x\|) \setminus B(x, \|y-x\|)\}|\bigg).
\end{aligned}$$

Note that

$$\begin{aligned}
p_1(x,y,t)p_2(x,y,t) = {}& \mathbf{1}[\|x-q'\| + \|y-x\| \geq t+l] p_1(x,y,t)p_2(x,y,t) \\
& + \mathbf{1}[\|x-q'\| + \|y-x\| < t+l] p_2(x,y,t). \qquad (22)
\end{aligned}$$

If $\|x-q'\|+\|y-x\|\geq t+l$, then $B(q,t)\subseteq B(q',t+l)\subseteq B(q',\|x-q'\|+\|y-x\|)$, and so

$$p_2(x,y,t)=\exp\left(-\rho\left[c(\|x-q'\|,t+l,\|y-x\|)-c(\|x-q\|,t,\|y-x\|)\right]\right). \tag{23}$$

If $\|x-q'\|+\|y-x\|<t+l$, then $B(x,\|y-x\|)\subseteq B(q',\|x-q'\|+\|y-x\|)\subseteq B(q',t+l)$ and $B(q,t)\subseteq B(q',t+l)$, and so if $A^c=\mathbb{R}^d\setminus A$ denotes the complement of a set $A\subseteq\mathbb{R}^d$,

$$\begin{aligned}
&|\{B(q',t+l)\setminus B(q,t)\}\setminus\{B(q',\|x-q'\|+\|y-x\|)\setminus B(x,\|y-x\|)\}|\\
&=|B(q',t+l)\cap B(q,t)^c\cap[B(q',\|x-q'\|+\|y-x\|)^c\cup B(x,\|y-x\|)]\,|\\
&=|B(q',t+l)\cap B(q,t)^c\cap B(q',\|x-q'\|+\|y-x\|)^c|\\
&+|B(q',t+l)\cap B(q,t)^c\cap B(x,\|y-x\|)|\\
&=\big[|B(q',t+l)|-|B(q,t)|-|B(q',\|x-q'\|+\|y-x\|)|\\
&+|B(q,t)\cap B(q',\|x-q'\|+\|y-x\|)|\big]+[|B(x,\|y-x\|)|-|B(q,t)\cap B(x,\|y-x\|)|]
\end{aligned} \tag{24}$$

Now, (21) follows from (19) and (22)-(24).

Denote $Z(x)$ the almost surely unique nearest point to x in $\{X_1,\ldots,X_M\}=\Psi\cup\{Z,X_M\}$ (so $Z(q)=Z$). By (12)-(14) and (D) in Section 3.1.2,

$$\begin{aligned}
\mathrm{P}(x\in\mathcal{R}|Z)=\;&\mathrm{P}(Z=Z(x),\,R_{M-1}<\|x-q'\|+\|Z-x\|\leq R_M|Z)\\
&+\mathrm{E}\left(\sum_{i=1}^{N}\mathbf{1}\left[X_i=Z(x),\,R_{M-1}<\|x-q'\|+\|X_i-x\|\leq R_M\right]\middle|Z\right).
\end{aligned} \tag{25}$$

By (iv) (above Theorem 1), with probability one,

$$Z=Z(x)\Leftrightarrow[\Psi\cup\{X_M\}]\cap B(x,\|Z-x\|)=\emptyset.$$

Conditional on Z, $R_M^d-(T+l)^d$ is exponentially distributed and independent of Ψ, cf. (ii) (above Theorem 1). Therefore, ignoring the null set where $\|Z-q'\|=\|x-q'\|+\|Z-x\|$ (i.e., $\|Z-q'\|<\|x-q'\|+\|Z-x\|$ almost surely),

$$\begin{aligned}
&\mathrm{P}(Z=Z(x),\,R_{M-1}<\|x-q'\|+\|Z-x\|\leq R_M|Z)\\
=&\mathrm{P}(\|x-q'\|+\|Z-x\|\leq R_M,\,X_M\notin B(x,\|Z-x\|)|Z)\\
&\mathrm{P}(\Psi\subset B(q',\|x-q'\|+\|Z-x\|)\setminus B(x,\|Z-x\|)|Z)\\
=&p_1(x,Z,T)p_2(x,Z,T),
\end{aligned} \tag{26}$$

using in the last equality that $\|x-q'\|+\|Z-x\| \leq R_M$ implies that $X_M \notin B(x, \|Z-x\|)$, since $B(x, \|Z-x\|) \subseteq B(q', \|x-q'\| + \|Z-x\|)$. Moreover,

$$
\begin{aligned}
&\mathrm{E}\left(\sum_{i=1}^{N} \mathbf{1}\left[X_i = Z(x),\, R_{M-1} < \|x-q'\| + \|X_i - x\| \leq R_M\right] \middle| Z\right)\\
=&\mathrm{E}\Bigg(\sum_{i=1}^{N} \mathbf{1}[[(\Psi \setminus \{X_i\}) \cup \{Z, X_M\}] \cap B(x, \|X_i - x\|) = \emptyset,\\
&(\Psi \setminus \{X_i\}) \cup \{Z\} \subset B(q', \|x-q'\| + \|X_i - x\|),\, \|x-q'\| + \|X_i - x\| \leq R_M] \Bigg| Z\Bigg)\\
=&\rho \int \mathbf{1}\left[y \in B(q', T+l) \setminus B(q, T),\, Z \in B(q', \|x-q'\| + \|y-x\|) \setminus B(x, \|y-x\|)\right]\\
&\mathrm{P}(\|x-q'\| + \|y-x\| \leq R_M,\, X_M \notin B(x, \|y-x\|)|Z)\\
&\mathrm{P}\left(\Psi \subset B(q', \|x-q'\| + \|y-x\|) \setminus B(x, \|y-x\|)|Z\right) \mathrm{d}y\\
=&\rho \int \mathbf{1}\left[y \in B(q', T+l) \setminus B(q, T),\, Z \in B(q', \|x-q'\| + \|y-x\|) \setminus B(x, \|y-x\|)\right]\\
&p_1(x, y|Z) p_2(x, y|Z)\, \mathrm{d}y, \qquad (27)
\end{aligned}
$$

using in the second equality the Slivnyak-Mecke formula for the Poisson process $\Phi \setminus \{Z\}$ conditional on Z [2, 7] (or see Theorem 3.2 in [4]), and using in the last equality a similar argument as when we obtained the last equality in (26). Finally, from (25)-(27) we obtain (20).

Recall that $p(x)$ is the probability that x belongs to the inferred privacy region. Clearly, $p(q) = 1$ since $q \in \mathcal{R}$. For $x \neq q$ and l fixed, both $p(x)$ and $\mathrm{E}(V)$ approach 0 as ρ tends to ∞. This follows by combining (15)–(17) and (19)–(20). It is interesting to study how $p(x)$ varies as a function of x when $d = 2$. Figure 3 plots the contours of $p(x)$ when $\rho = 1$ and $l = 1$. Observe that contours with high $p(x)$ are located close to the point $q = (1, 0)$. Contours with low $p(x)$ appear as circle-like shapes, with centre $q' = (0, 0)$ and in pairs, with radii below 1.0 and above 1.0, respectively. Figure 4 shows the contours of $p(x)$ when $\rho = 10$ and $l = 1$. This function resembles that of Figure 3, except that the region with high $p(x)$ is shrinked significantly.

Two methods are employed to evaluate $\mathrm{E}(V)$ when $d = 2$. Again we take $q' = (0, 0)$ and $q = (l, 0)$. The first method is *Monte Carlo*, which executes 10,000 instances of the radial simulation algorithm in Section 2.1.2 until the termination time M is determined. For each simulation, we estimate the area of V by using an 100×100 square grid over

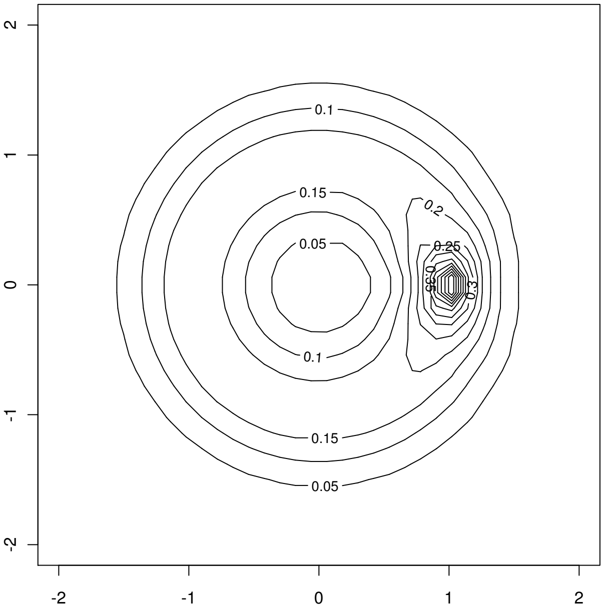

FIGURE 3: Contours of $p(x)$, when $\rho = 1$, $l = 1$, and $d = 2$.

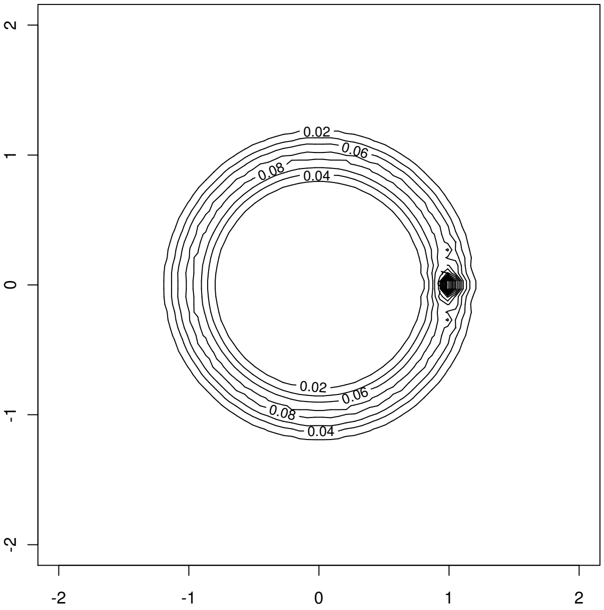

FIGURE 4: Contours of $p(x)$, when $\rho = 10$, $l = 1$, and $d = 2$.

the domain $[-R_M, R_M]^2$ which contains $\mathcal{R}$. The value of $\mathrm{E}(V)$ is then estimated by the average area obtained from all simulations. The second method is *numeric integration*, using the following setting when $l = 1$ and $\rho = 1, 2, 5, 10, 20, 50, 100$.

- The integral in (20) is computed by using a 100×100 square grid in the region $[-(t+l), (t+l)]^2$. All possible points y such that the indicator function in (20) is equal to one must be located inside such a region.
- The integral in $p(x) = \int p(x|z) f(z) \, \mathrm{d}z$ is computed by using a 100×100 square grid in the region $[-3l, 3l]^2$. In fact $p(x)$ is effectively zero outside this region and seemingly only limited value is lost even though the full space $\mathbb{R}^2$ is not used as the domain for numeric integration.
- For $\rho = 1, 2, 5, 10, 20, 50$, the integral in $\mathrm{E}(V) = \int p(x) \, \mathrm{d}x$ is computed by using a 100×100 square grid in the region $[-3l, 3l]^2$. Like above, only limited value is lost when $[-3l, 3l]^2$ is used as the bounding region. For $\rho = 100$, after first using the same method and comparing with the Monte Carlo estimate, we found it appropriate to use polar coordinates (θ, r) for x and a 100×100 square grid for (θ, r) in the domain $[0, 2\pi) \times [0.75, 1.25)$. Outside this domain $p(x)$ is almost zero.

Figure 5a shows $\mathrm{E}(V)$ as a function of ρ when $l = 1$ and $d = 2$. Observe that the value obtained by numeric integration is close to the corresponding value obtained by Monte Carlo. Figure 5b plots $\mathrm{E}(V)$ as a function of l when $\rho = 1$ and $d = 2$. This plot is just obtained from the results in Figure 5a using (18). For $\rho = 100$, the difference between the values obtained by numeric integration and Monte Carlo becomes more visible (the estimates of $\mathrm{E}(V)$ when $(\rho, l) = (100, 1)$ and obtained using a square grid for respective x and its polar coordinates are 0.0160 and 0.0182 as compared to the Monte Carlo estimate 0.0176). Note that $\mathrm{E}(V)$ appears to be an increasing function of l, with a decreasing slope.

Acknowledgements

Supported by the Danish Natural Science Research Council, grants 272-06-0442 and 09-072331, "Point process modelling and statistical inference".

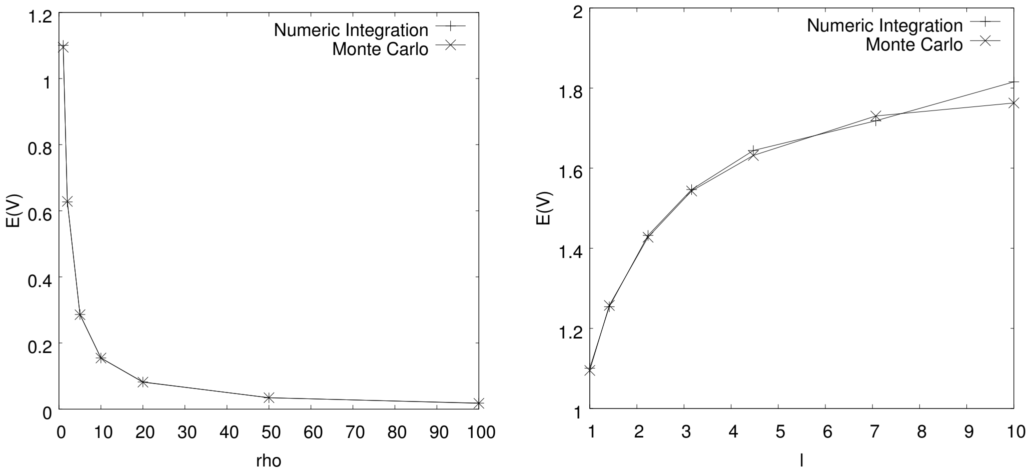

(a) E(V) vs. ρ, when $l = 1$.

(b) E(V) vs. l, when $\rho = 1$.

FIGURE 5: Evaluation of E(V).

References

[1] KINGMAN, J. F. C. (1993). *Poisson Processes.* Clarendon Press, Oxford.

[2] MECKE, J. (1967). Stationäre zufällige Maße auf lokalkompakten Abelschen Gruppen. *Zeitschrift für Wahrscheinlichkeitstheorie und verwandte Gebiete* **9,** 36–58.

[3] MØLLER, J. (1994). *Lectures on Random Voronoi Tessellations.* Lecture Notes in Statistics 87. Springer-Verlag, New York.

[4] MØLLER, J. AND WAAGEPETERSEN, R. P. (2004). *Statistical Inference and Simulation for Spatial Point Processes.* Chapman and Hall/CRC, Boca Raton.

[5] OKABE, A., BOOTS, B. AND SUGIHARA, K. (1992). *Spatial Tessellations. Concepts and Applications of Voronoi Diagrams.* Wiley, Chichester.

[6] QUINE, M. P. AND WATSON, D. F. (1984). Radial generation of n-dimensional Poisson processes. *Journal of Applied Probability* **21,** 548–557.

[7] SLIVNYAK, I. M. (1962). Some properties of stationary flows of homogeneous random events. *Teor. Veroyat. Primen.* **7,** 347–352. (in Russian). English translation: Theory Prob. Appl. 7, 336-341.

[8] Stoyan, D., Kendall, W. S. and Mecke, J. (1995). *Stochastic Geometry and Its Applications* second ed. Wiley, Chichester.

[9] Yiu, M. L., Jensen, C. S., Huang, X. and Lu, H. (2008). SpaceTwist: Managing the trade-offs among location privacy, query performance, and query accuracy in mobile services. In *Proceedings of the 24th IEEE International Conference on Data Engineering*. ed. M. Castellanos, A. P. Buchmann, and K. Ramamritham. IEEE Computer Society, Los Alamitos, CA. pp. 366–375.

[10] Yiu, M. L., Jensen, C. S., Møller, J. and Lu., H. (2009). Design and analysis of an incremental approach to location privacy for location-based services. Submitted.